Laemmli, U. K. (1970) *Nature (London) 227*, 680-685.
Montreuil, J. (1980) *Adv. Carbohydr. Chem. Biochem. 37*, 157-213.
Plummer, T. H., Jr., & Tarentino, A. L. (1981) *J. Biol. Chem. 256*, 10243-10246.
Plummer, T. H., Jr., Elder, J. H., Alexander, S., Phelan, A. W., & Tarentino, A. L. (1984) *J. Biol. Chem. 259*, 10700-10704.
Putnam, F. W., Florent, G., Paul, C., Shinoda, T., & Shimizu, A. (1973) *Science (Washington, D.C.) 182*, 287-291.
Schmid, K., Kaufman, H., Isemura, S., Bauer, F., Emura, J., Motoyama, T., Ishiguro, M., & Nanno, S. (1973) *Biochemistry 12*, 2711-2724.
Taga, E. M., Waheed, A., & Van Etten, R. L. (1984) *Biochemistry 23*, 815-822.
Takahashi, N., & Nishibe, H. (1978) *J. Biochem. (Tokyo) 84*, 1467-1473.
Takahashi, N., & Nishibe, H. (1981) *Biochim. Biophys. Acta 657*, 457-467.
Tarentino, A. L., & Maley, F. (1974) *J. Biol. Chem. 249*, 811-817.
Tarentino, A. L., & Galivan, J. (1980) *In Vitro 16*, 833-846.
Tarentino, A. L., & Plummer, T. H., Jr. (1982) *J. Biol. Chem. 257*, 10776-10780.
Tarentino, A. L., & Plummer, T. H., Jr. (1984) *Fed. Proc., Fed. Am. Soc. Exp. Biol. 43*, 1552.
Tarentino, A. L., Trimble, R. B., & Maley, F. (1978) *Methods Enzymol. 50*, 574-580.
Warburg, O., & Christian, W. (1941) *Biochem. Z. 310*, 384-421.

NMR Structural Analysis of a Membrane Protein: Bacteriorhodopsin Peptide Backbone Orientation and Motion†

B. A. Lewis,‡,§ G. S. Harbison,‖ J. Herzfeld,‖ and R. G. Griffin*,‡

Francis Bitter National Magnet Laboratory, Massachusetts Institute of Technology, Cambridge, Massachusetts 02139, and Department of Physiology and Biophysics, Harvard Medical School, Boston, Massachusetts 02115

Received January 7, 1985

ABSTRACT: In reconstituted vesicles above the lipid phase transition temperature, bacteriorhodopsin (BR) undergoes rotational diffusion about an axis perpendicular to the plane of the bilayer [Cherry, R. J., Muller, U., & Schneider, G. (1977) *FEBS Lett. 80*, 465]. This diffusion narrows the ^{13}C NMR powder line shape of the BR peptide carbonyls. In contrast, BR in native purple membrane is relatively immobile and exhibits a rigid-lattice powder line shape. By use of the principal values of the rigid-lattice chemical shift tensor and the motionally narrowed line shape from the reconstituted system, the range of Euler angles of the leucine peptide groups relative to the diffusion axis has been calculated. The experimentally observed line shape is inconsistent with those expected for structures which consist entirely of either α helix or β sheet perpendicular to the membrane or β sheet tilted at angles up to about 60° from the membrane normal. However, for two more complex structural models, the predicted line shapes agree well with the experimental one. These are, first, a structure consisting entirely of α_I helices tilted at 20° from the membrane normal and, second, a combination of 60% α_{II} helix perpendicular to the membrane plane and 40% antiparallel β sheet tilted at 10-20° from the membrane normal. The results also indicate that the peptide backbone of bacteriorhodopsin in native purple membrane is extremely rigid even at 40°. The experiments presented here demonstrate a new approach, using solid-state nuclear magnetic resonance (NMR) methods, for structural studies of transmembrane proteins in fluid membrane environments, either natural or reconstituted. Analysis of NMR powder line shapes which are narrowed by anisotropic rotational diffusion can provide information not only on secondary structure but also, in general, on the orientation of labeled groups relative to the axis of rotational diffusion. Such information on the orientation of membrane proteins in the bilayer plane is difficult to obtain by more conventional structural methods.

Membrane proteins have been notoriously difficult subjects for structural investigations. Because they rarely form well-ordered three-dimensional crystals, conventional high-resolution crystallographic methods have not been generally applicable. When two-dimensional crystals are available, the electron microscopic methods pioneered by Henderson & Unwin (1974) for three-dimensional reconstruction can be used, but to date, technical limitations have prevented the determination of such structures at atomic resolution. Another technique which has recently been applied to the structural analysis of proteins involves the use of two-dimensional solution nuclear magnetic resonance (NMR)[1] [see, for example, Wagner & Wuthrich (1982)]. However, most integral mem-

† This research was supported by the National Institutes of Health (GM-23289, GM-23316, and RR-00995) and the National Science Foundation through its support of the Francis Bitter National Magnet Laboratory (DMR-8211446). B.A.L. is the recipient of a U.S. Public Health Service postdoctoral fellowship (GM-09062).

‡ Massachusetts Institute of Technology.
§ Present address: Biology Division, Oak Ridge National Laboratory, Oak Ridge, TN 37830.
‖ Harvard Medical School.

[1] Abbreviations: BR, bacteriorhodopsin; DMPC, 1,2-dimyristoylphosphatidylcholine; DPPC, 1,2-dipalmitoylphosphatidylcholine; MASS, magic-angle sample spinning; NMR, nuclear magnetic resonance; SDS, sodium dodecyl sulfate; NOE, nuclear Overhauser effect; Me_4Si, tetramethylsilane.

0006-2960/85/0424-4671$01.50/0

brane proteins do not yield high-resolution solution NMR spectra, making this method again inapplicable. To study membrane proteins by NMR, it is thus more appropriate to use solid-state methods which are designed to deal with the broad NMR spectra obtained from samples in anisotropic media.

In this paper, we report on the use of solid-state NMR to obtain a particular type of structural information on a membrane protein, namely, the orientation of certain molecular groups relative to the plane of the membrane bilayer. These experiments utilize the fact that in many biological membranes, and in reconstituted vesicles with sufficiently high lipid:protein ratios, integral membrane proteins diffuse rapidly about an axis normal to the plane of the membrane (Edidin, 1974). Such rapid diffusion about a locally defined axis in a "powder" (randomly oriented) sample produces motionally averaged NMR line shapes which depend on the angles between the principle axes of the chemical shift (or quadrupolar or dipolar) tensor and the diffusion axis. Thus, the experimental line shape can be interpreted in terms of the orientation of the observed groups with respect to the diffusion axis. This structural information is similar to that obtained from oriented samples [for examples, see Griffin et al. (1978) and Cross & Opella (1983)] but is more generally applicable, requiring neither the orientation of the sample nor the dehydration frequently required to achieve orientation. In principle, this method can be used with any membrane protein which undergoes rapid rotational diffusion; isotopic labeling is also desirable but not strictly required. A similar approach has recently been taken by Pauls et al. (1984), who have used deuterium NMR to examine both orientation and rotational motion of exchangeable hydrogen positions in an α-helical polypeptide in DPPC bilayers.

Bacteriorhodopsin (BR) is highly immobilized in its native purple membrane (Razi-Nagvi et al., 1973). However, when BR is reconstituted with additional lipid and observed at temperatures at which these lipids are in the "liquid-crystalline" (L_α) phase, it executes rotational diffusion with a value for the rotational diffusion coefficient $D_R \simeq (5\text{–}10) \times 10^4\ s^{-1}$ at a sufficiently high lipid:protein ratio (Peters & Cherry, 1982; Cherry & Godfrey, 1981). This corresponds to a correlation time $\tau_c = 1/6D_R \simeq 2\text{–}3\ \mu s$. On the other hand, at temperatures below the lipid main phase transition temperature (T_m), the diffusion slows below the limit of detection by optical methods (Cherry et al., 1978; Hoffman et al., 1980). In the present experiment, the peptide carbonyl carbons of the 36 leucines of BR have been ^{13}C labeled, and reconstituted vesicles have been prepared by adding DMPC to the labeled purple membranes. Since the T_m of DMPC is 23 °C, the rotational correlation time of the protein should vary over several orders of magnitude in the temperature range from 0 to 30 °C. Since the peptide carbonyl tensor is about 12 kHz wide at the magnetic field strengths used here (6.9 and 7.4 T), motions with correlation times much shorter than about 13 μs will be in the fast limit. Thus, at temperatures above 23 °C, the ^{13}C spectra for the peptide-labeled BR will be motionally narrowed and can be interpreted in terms of the orientation(s) of the peptide backbone relative to the membrane normal. Under ideal conditions, this information can help to distinguish among models for the secondary structure of such a membrane protein. In addition, the NMR spectrum of the labeled BR in native purple membrane provides information on the degree of motion of the peptide backbone in situ.

BR is particularly well suited for these experiments since several types of evidence point to the existence of highly ordered secondary structure [for reviews, see Henderson (1977), Wallace (1982), and Stoeckenius & Bogomolni (1982)]. For example, the three-dimensional structure obtained from electron diffraction (Henderson & Unwin, 1974) shows seven rods of density whose axes all lie within about 20° of the membrane normal, and Fourier-transform infrared absorption spectroscopy results are consistent with oriented α helices for which the average tilt angle is 26° or less (Rothschild et al., 1982). However, there is not yet universal agreement on the structural details. Most investigators presently support the view that BR contains seven transmembrane α helices but others contend that a substantial amount of the density observed in electron diffraction maps can be better accounted for by up to four β strands which are tilted at about 10–15° from the membrane normal (Jap et al., 1983). Thus, additional information on the orientation of the peptide bonds in BR may be useful. One reason for choosing to label the leucines here is that the all-helical models predict that about 90% of the leucines are in the helices [for example, see Engelman et al. (1982), Khorana et al. (1979), and Ovchinnikov et al (1979)], while the suggestions of Jap et al. (1983) place only 54% of the leucines in helices and 33% in the β sheet. These two cases should be distinguishable by experiments, such as those described here, which provide a new way of determining peptide bond orientations in a membrane protein.

Materials and Methods

Halobacterium halobium strain R1 was grown in a defined growth medium (Argade et al., 1981) with L-[1-^{13}C]leucine (Cambridge Isotope Labs) at a concentration of 0.08 g/L. Purple membrane was isolated by the method of Oesterhelt & Stoeckenius (1974). Radiotracer experiments showed a high specificity of labeling. First, upon ammonia–acetone extraction, 98% of the counts were recovered in the protein fraction vs. 2% in the lipid–retinal fraction. Second, amino acid analysis of the protein showed no counts above background in amino acids other than leucine.

SDS gel electrophoresis of the native membrane showed a single band at the correct position for intact BR. Thus, there was no detectable proteolytic degradation of BR; more specifically, at least 95% of the BR molecules had an intact C terminus. To look for possible aggregation of the purple membrane fragments, a portion of one NMR sample was diluted, stained with uranyl acetate, and examined by transmission electron microscopy (EM). Although a small amount of aggregation was present, at least 80% of the membrane fragments were monodisperse so that most of the membrane surface was not in contact with other surfaces. Thus, although the membranes were relatively tightly packed in the pellet used for the NMR experiments, they did not irreversibly aggregate. These NMR samples are generally about 20 wt % membrane and thus contain a substantial water layer between neighboring membrane fragments.

Reconstituted vesicles were made by the method of Cherry et al. (1978). Thirty-three milligrams of purple membrane (containing 25 mg of BR) was solubilized for 24 h in 132 mL of 0.1% Triton X-100 (Sigma) and 0.1 M sodium acetate, pH 5. Ninety-two milligrams of DMPC (Calbiochem) was lyophilized from benzene–methanol and added to the purple membrane–Triton solution, which was stirred gently until clear. The mixture was dialyzed against 0.1 M sodium acetate and 0.02% sodium azide at 4 °C for 10 days with several changes. The reconstituted vesicles were centrifuged through a 5–40% (w/v) sucrose gradient, washed with distilled water, and concentrated by centrifugation for the NMR experiments. The entire preparation, with the exception of the sucrose gradient

which was deemed to be unnecessary, was carried out a second time with identical NMR results; the data presented here are from the second sample.

For both native membrane and reconstituted vesicles, the NMR samples were prepared by centrifugation and subsequent transfer of the pellet to 6-mm glass tubes. The samples were sealed with parafilm (American Can Co., Greenwich, CT) which will contribute a ^{13}C NMR signal in the upfield region of the spectrum but not in the carbonyl region.

^{13}C powder NMR spectra were taken on a home-built spectrometer operating at 74.2 MHz for ^{13}C and at 294.9 MHz for ^{1}H (6.9 T). For cross-polarization, a proton H_1 of 40 kHz was used while for single-pulse and Hahn echo (90°–τ–180°) sequences the ^{13}C 90° pulse was 5.1 μs. A delay of τ = 40 μs was used in the echo sequences, and phase cycling and high-power (dipolar) decoupling were used throughout. Recycle delays were 2 s for cross-polarization and 10–80 s for the Hahn echo and single-pulse experiments.

The MASS spectra were taken on a home-built spectrometer with a 7.4-T magnet, using aluminum oxide rotors in a double air bearing stator system (Doty Scientific, Columbia, SC). Typical radio-frequency fields were equivalent to 50 kHz for cross-polarization and 100 kHz for decoupling. Cross-polarization spectra were obtained by standard methods, with recycle delays of 4 s. Single-pulse experiments were conducted in the usual manner, except that the proton spin system was kept saturated during the (20 s) recycle by applying a 90° pulse every 0.5 ms. This gave a uniform enchancement of approximately 2.5 over a standard gated decoupling spectrum, presumably because the dominant relaxation mechanisms of rigid carbons is by spin diffusion to rapidly relaxing methyls which have a high NOE [cf. Szeverenyi et al. (1982)]. Shift tensor principal values were obtained from the integrated intensities by using the method of Herzfeld & Berger (1980) at five different spinning speeds.

Results

Native Purple Membrane. Figure 1a shows the ^{13}C NMR spectrum of an ultracentrifuge pellet of native [^{13}C]leucine-labeled purple membrane. This spectrum was obtained with cross-polarization followed by an echo pulse. From the carbonyl powder pattern (left side of the spectrum) and from magic-angle spinning data (see below), the principal values of the ^{13}C leucine chemical shift tensor are 246 ± 1, 191 ± 2, and 93 ± 1 ppm from Me_4Si. The isotropic chemical shift is 176 ppm, which is consistent with hydrogen-bonded peptide carbonyls, as expected if most of the protein has a regular secondary structure. The width (153 ppm) of the tensor is very close to that for the peptide carbonyl in crystalline Gly·Gly·HCl·H_2O (Stark et al., 1983). This width and the relatively well-defined edges of the carbonyl powder pattern indicate that no backbone motions larger than about 10° and faster than 100 s^{-1} are present. It should be noted that all the samples used in this work were very concentrated ultracentrifuge pellets. Thus, overall motion of the membrane fragments or vesicles is strongly restricted, and any motional averaging observed is due to local motions of the protein.

The static line shape is formally a convolution of the ^{13}C chemical shift and the ^{13}C–^{14}N dipolar tensors. However, the latter interaction is much smaller than the former [$D_\perp(^{13}C$–$^{14}N) \simeq 635$ Hz] and is manifest only as a broadening in the powder spectra.

The spectrum shown in Figure 1a was taken at 3 °C, but identical spectra were obtained at 25 and 40 °C, showing that no additional motion occurs even at the growth temperature

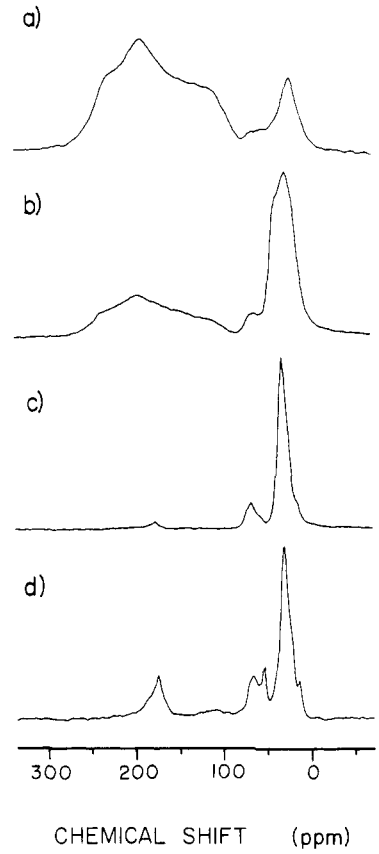

FIGURE 1: ^{13}C NMR powder spectra of samples with [1-^{13}C]-leucine-labeled BR. Samples were all ultracentrifuge pellets. The labeled carbonyl spectra are on the left sides of the figures; on the right are resonances of most other carbons at natural abundance. (a) Hydrated native purple membrane at 3 °C. Taken with cross-polarization and a subsequent refocusing (180°) pulse. Mixing time, 2 ms; recycle delay, 2 s; 300-Hz line broadening. (b) Reconstituted BR–DMPC vesicles at 3 °C. Same conditions as (a) except 200-Hz line broadening. (c) Reconstituted vesicles at 30 °C. Same conditions as (b). (d) Reconstituted vesicles at 30 °C. Taken with a Hahn echo (90°–τ–180°) sequence with τ = 40 μs. Recycle delay, 10 s; 200-Hz line broadening.

of *H. halobium*. The lack of motion is expected given the crystalline packing of BR in the purple membrane and is consistent with previous results of transient dichroism studies (Razi-Naqvi et al., 1973). However, the present results go beyond previous work since they demonstrate that in hydrated purple membrane the peptide backbone of BR is immobile within the protein, in addition to the restriction of motion of the chromophore and protein as a whole. The rigidity of the peptide backbone in BR contrasts with the librational motion observed for the peptide carbonyls in collagen (Sarkar et al., 1983) and the substantial motional averaging observed in myosin (Eads & Mandelkern, 1984). On the other hand, the coat protein of the bacteriophage fd also has a rigid peptide backbone, as shown by solid-state NMR (Cross & Opella, 1982).

An important consideration when using cross-polarization is the fact that the efficiency of cross-polarization can decrease markedly in the presence of molecular motion (Pines et al., 1972). Therefore, it is possible to suppress signals from mobile parts of BR relative to those from rigid carbons. To test for the presence of more mobile leucines, data on the native purple membrane sample were also taken with a single 90° pulse and with a Hahn echo sequence (data not shown). In neither case were any sharp features observed, ruling out the presence of rapid large-amplitude motion at any of the 36 leucine sites in BR.

Reconstituted Vesicles. Shown in Figure 1b is the cross-polarization NMR spectrum of the reconstituted [^{13}C]-leucine-labeled BR–DMPC vesicles at 3 °C, well below the main phase transition temperature (T_m) of the lipid. This is also a rigid-lattice spectrum, and the edges correspond exactly to those of the native purple membrane spectrum. This is not surprising since Cherry et al. (1978) have shown that in such vesicles below T_m, BR aggregates and forms a crystalline lattice very similar to that of native purple membrane. Furthermore, transient dichroism experiments show that BR is immobilized under these conditions (Cherry et al., 1978; Hoffman et al., 1980). As for the native membrane, spectra were also taken with a Hahn echo sequence to look for more mobile carbonyls which might not cross-polarize well. Again, sharp features, indicative of rapid isotropic motion, were not observed.

In reconstituted DMPC vesicles above the lipid T_m, BR is monomeric and undergoes rapid rotational diffusion (Cherry et al., 1978; Hoffman et al., 1980). This diffusion is highly anisotropic and is well represented by motion about an axis perpendicular to the plane of the bilayer with very little "wobble" (Cherry & Godfrey, 1981). ^{13}C NMR spectra of the BR–DMPC vesicles at 30 °C, 7 °C above the T_m, are shown in Figure 1c,d. The trace in Figure 1c was obtained by using the same cross-polarization conditions as in Figure 1a,b. A much narrower powder pattern, as expected for a motionally averaged carbonyl tensor, is seen, but at very low intensity compared to that in Figure 1b; this indicates that the cross-polarization efficiency has decreased with the onset of rotational diffusion. In fact, at least some of the carbonyl intensity observed in Figure 1c may be due to the lipid carbonyls at natural abundance. The spectrum of Figure 1d, obtained by using a Hahn echo sequence with a recycle delay of 10 s, more clearly shows the motionally averaged BR carbonyl line shape. This region will contain contributions from the other BR peptide groups and the DMPC carbonyls at natural abundance, but each of these should only represent about 5% of the leucine carbonyl intensity. For the DMPC carbonyls, in particular, the relative intensity measured from the magic-angle spinning spectrum (see below) is about 18:1 (leucine:DMPC).

The width of the motionally averaged carbonyl spectrum at half-height is 18 ppm, with the maximum upfield (to the right) of the isotropic frequency; 90% of the intensity is within a width of 31 ppm. The implications of this line shape for the orientation of the peptide backbone in BR, and thus its secondary structure, will be discussed in the next sections. The line shape did not change with recycle delay, showing that the spin–lattice relaxation time (T_1) is orientationally isotropic. Measurement of the intensity as a function of recycle delay (progressive saturation) yielded a value for T_1 of approximately 10–15 s. These measurements required several hours of data acquisition and were performed only after acquisition of the original spectrum.

Line-Shape Analysis. The approach used here is twofold. First, we determine the range of orientations of the leucine peptide groups which are consistent with the observed motionally averaged ^{13}C line shape. Second, we note which of the possible secondary structures for BR would result in peptide orientations within this range, and we consider the effects on the line shape of tilting of α helices and β sheets. It is assumed that no wobble occurs. To have a significant effect on the line width, angular fluctuations of greater than about ±20° about the diffusion axis would have to occur, and the analysis of Cherry & Godfrey (1981) suggests that wobble of such amplitude would have been detectable in the transient dichroism data.

Fast-limit motion about a unique axis will produce a powder pattern which is axially symmetric, regardless of whether the rigid-lattice spectrum is axially symmetric or asymmetric. The exact shape (the width and sign of the anisotropy) of such a motionally averaged powder pattern is determined by the three principal values of the rigid-lattice shift tensor, σ_{ii}, and their orientation with respect to the diffusion axis. Specifically, the breadth of the motionally averaged tensor $\Delta\sigma^R = \sigma_\parallel^R - \sigma_\perp^R$ is given by

$$\Delta\sigma^R = \tfrac{1}{2}(3\cos^2\beta - 1)[\sigma_{33} - \tfrac{1}{2}(\sigma_{11} + \sigma_{22})] + \tfrac{3}{4}(\sigma_{11} - \sigma_{22})\sin^2\beta\cos 2\alpha$$

(Mehring et al., 1971) where α and β are the Euler angles relating σ_{ii} to the diffusion axis [see Mehring (1983) for a complete discussion].

For an axially symmetric rigid-lattice tensor, a unique line shape results from rotational diffusion characterized by a given angle β. Unfortunately, the same is not true for an axially asymmetric rigid-lattice tensor. That is, a given line shape does not imply a unique pair of angles but can result from a range of possible orientations. Nevertheless, a much larger set of orientations can generally be ruled out. For a random distribution of 36 peptide bond orientations in a protein, the line shape resulting from fast rotational diffusion about a particular axis would be a superposition of 36 different powder patterns, but if most of the orientations fall within a limited range, then a more well-defined NMR spectrum would be observed. Current structural information suggests that BR falls into the latter category, consisting mainly of helices and possibly a few strands of β sheet, all with their axes close to colinear with the membrane normal.

For the analysis here, it is assumed that the chemical shift tensors of the peptide carbons of all 36 leucines in BR are identical and that their principal axes have the same local orientation as found in crystals of the dipeptide Gly·Gly·HCl·H_2O (Stark et al., 1983). Specifically, σ_{11} and σ_{22} lie in the plane of the peptide bond and form angles of 77° and 13°, respectively, with the C=O bond, while σ_{33} is perpendicular to the peptide bond plane (see Figure 3). By use of the principal values of the rigid-lattice chemical shift tensor obtained from native purple membrane, $\Delta\sigma^R$ has been calculated as a function of the Euler angles α and β. The results are shown in Figure 2a, and the range of angles consistent with the experimental results is apparent.

Since the perpendicular edge of the experimental powder pattern is upfield of the isotropic frequency, $\Delta\sigma$ must be positive for essentially all orientations present in the sample. Using the position of the maximum and the limits within which lies 90% of the intensity, we conclude that most of the components lie between $\Delta\sigma = +8$ and $+31$. Thus, the range of leucine peptide carbonyl orientations in this sample encompasses approximately the following sets of Euler angles (in degrees): $\beta = 50$, $\alpha = 0$–20; $\beta = 60$, $\alpha = 30$–50; $\beta = 70$, $\alpha = 50$–80; $\beta = 80$, $\alpha = 65$–90; $\beta = 90$, $\alpha = 75$–90. A few (roughly 10–15%) of the peptide groups are at angles outside this range, giving the trailing edges of the experimental spectrum with 31 ppm $< \Delta\sigma <$ 56 ppm. At least some of this intensity may result from intrinsic line broadening and chemical shift heterogeneity. For these Euler angles, the ^{13}C–^{14}N dipolar coupling is scaled by a factor of 2 or more, making it less than 300 Hz. Also, the very large asymmetric ^{14}N–peptide quadrupolar tensor causes ^{14}N to be relaxed very efficiently, even by the relatively slow rotational diffusion of

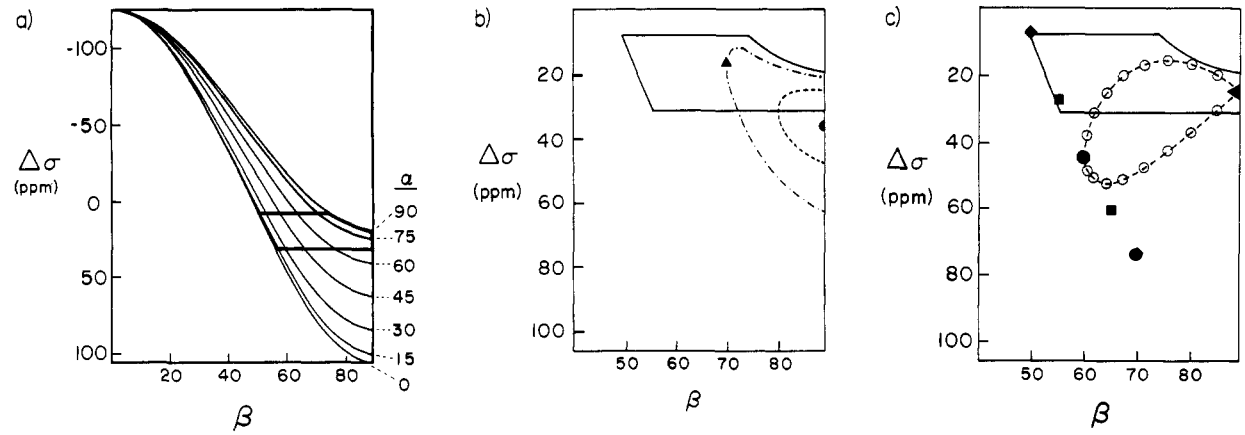

FIGURE 2: Plots of breadth of rotationally averaged line shape ($\Delta\sigma \equiv \sigma_{\parallel} - \sigma_{\perp}$) as a function of the Euler angles α and β for the [^{13}C]leucyl peptide group. (a) Full range of Euler angles. The heavy solid line outlines the allowed region ($8 < \Delta\sigma < 31$ ppm). (b) Expanded plot for $\Delta\sigma > 0$ showing the allowed range from the experimental line shape and calculated values for α helices. For tilted helices, the actual line shape will be a sum of several (up to 18 in principle) subspectra along one of the dotted lines. (●) α_I helix perpendicular to membrane plane; (–·–) α_I helix tilted at 10°; (– – –) α_I helix tilted at 20°; (▲) α_{II} helix perpendicular to membrane. (c) Expanded plot as in (b), showing the allowed region and calculated values for the antiparallel β sheet. For sheet tilted at all angles except 90°, the spectrum will be a sum of two subspectra. (●) β sheet with axis perpendicular to membrane plane. (■) β sheet tilted 5° about an axis perpendicular to the sheet axis and parallel to the peptide bond planes (i.e., the y axis in Figure 3b). The spectrum will be a sum of the two subspectra represented by the same symbols. (♦) β sheet tilted 10° as above. (○) β sheet tilted about an axis perpendicular to the sheet axis and perpendicular to the average of the peptide bond planes (i.e., about the x axis in Figure 3c). Each vertically related pair of symbols represents a 10° increment in the tilt angle (increasing from left to right). The spectrum will be a sum of the two subspectra represented by vertically related symbols (i.e., with the same value for β). (▲) β sheet tilted 90° as above, i.e., with sheet axis parallel to the membrane plane and peptide bond planes perpendicular to the membrane plane.

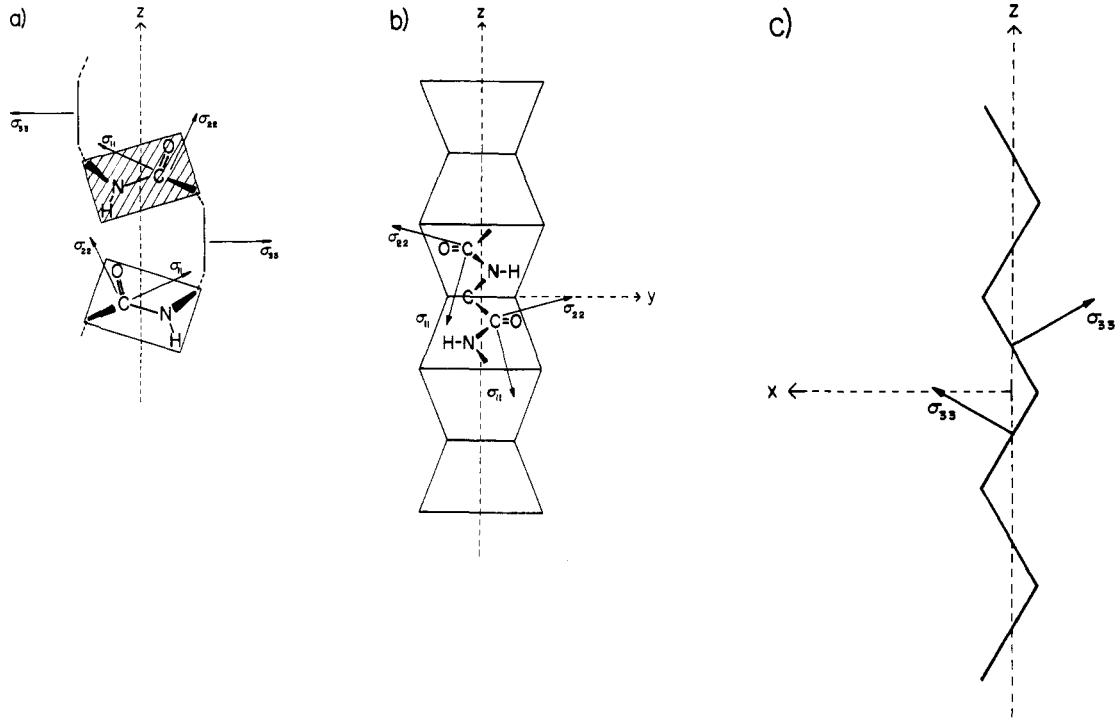

FIGURE 3: Schematic drawings of secondary structure elements. (a) Idealized α_I helix with 4.0 rather than 3.6 residues per turn. (b and c) Antiparallel β sheet (front and side views).

the protein. Calculations based on the expression given by Torchia & Szabo (1982) suggest that the ^{14}N T_1 is probably quite short and therefore is effectively "self-decoupled" from the carbon. Thus, it is not unexpected that we see no effects arising from ^{13}C–^{14}N coupling.

Secondary Structure Analysis. In this section, a number of possible models for the structure of BR are considered, and for each model, the predicted value for $\Delta\sigma$ and the predicted ^{13}C NMR line shape are compared with those experimentally observed for BR in DMPC vesicles. Three types of secondary structures which have been frequently suggested in discussions of the BR structure—α_I helix, α_{II} helix, and antiparallel β sheet—are included, and the models are examined in order of increasing complexity.

Schematic structures for α_I helix and antiparallel β sheet are shown in Figure 3. In an α_I helix (Figure 3a), the peptide bond planes are roughly parallel to the helix axis, and the C=O bond direction is a few degrees from it, while in antiparallel β sheet (Figure 3b,c) the peptide bond planes form angles of about 30° to the long axis of the sheet and the C=O bonds are roughly perpendicular to this axis. The α_{II} helix, suggested by Krimm & Dwivedi (1982) as a possible structural

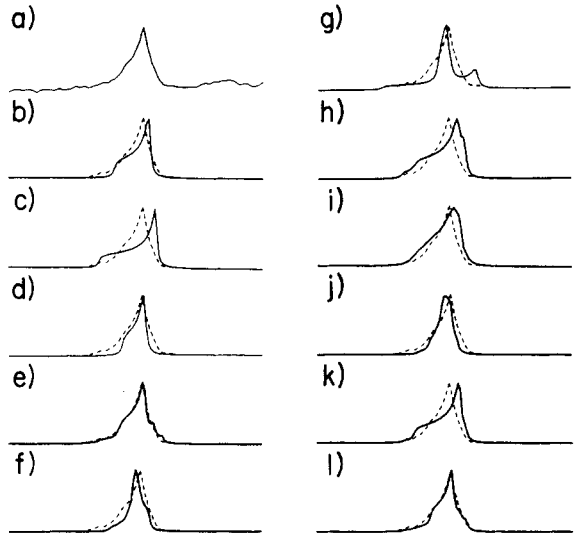

FIGURE 4: (a) Experimental spectrum for [^{13}C]leucine-labeled BR rotationally averaged by diffusion about the membrane normal (expansion of Figure 1d). (b–l) Calculated line shapes using a three-site jump model with a jump rate of 10^6 s^{-1}. All were calculated with 100-Hz line broadening. Dashed lines denote experimental spectra. (b) α_I helix oriented perpendicular to the membrane plane (α = 115°, β = 90°). (c) Antiparallel β sheet oriented perpendicular to the membrane plane (α = 13°, β = 60° or α = 193°, β = 300°). (d) α_{II} helix oriented perpendicular to the membrane plane (α = 115°, β = 110°). (e) α_I helix tilted at 20° from the membrane normal. Sum of eight subspectra. (f) α_{II} helix tilted at 10° from the membrane normal. Sum of eight subspectra. (g) β sheet tilted at 10° about an axis perpendicular to the sheet axis and parallel to the peptide bond planes (i.e., the y axis in Figure 3b). (h) β sheet tilted at 10–20° about an axis perpendicular to the average of the peptide bond planes (i.e., the x axis in Figure 3c). Sum of four subspectra, two for the 10° tilt and two for the 20° tilt. (i) Sum of subspectra for seven α_I helices, three perpendicular to the membrane plane, two tilted at 10°, and two tilted at 20°. (j) Sum of subspectra for seven α_{II} helices, oriented as in (i). (k) Mixed structure consisting of 60% α_I helix, perpendicular to the membrane plane, and 40% β sheet tilted at 10–20° as in (h). (l) Mixed structure as in (k) but with 60% α_{II} helix instead of α_I helix.

element in BR, is similar to the α_I helix except that the peptide bond planes are tilted outward from the helix axis; thus, in Figure 3a, σ_{33} for α_{II} helix will be tilted down from the position shown for α_I helix. In the following analysis, the choices of Euler angles for each structure are approximate; a detailed analysis of known protein structures will be performed in conjunction with further experiments using other NMR labels.

First, we consider models consisting entirely of one secondary structure type for which the axes are exactly perpendicular to the membrane plane. For α_I helix in this case, the peptide groups will all have Euler angles of approximately β = 90° and α = 115° (equivalent to 65° in the equation for $\Delta\sigma$). The plot of Figure 2a has been expanded in Figure 2b,c to focus on the "allowed" region (solid lines) between 8 and 31 ppm, and the predicted $\Delta\sigma$ for the transmembrane α_I helix (i.e., that perpendicular to the bilayer plane) is shown by the filled semicircle in Figure 2b. The calculated NMR line shape for this case is presented in Figure 4b. For the transmembrane β sheet, the two sets of peptide groups have Euler angles of approximately β = 60°, α = 13° and β = 300°, α = 193°, which give the same value for $\Delta\sigma$. This case is shown by the filled circle in Figure 2c, and its line shape is given in Figure 4c. The predicted $\Delta\sigma$ is further outside the allowed region than for the transmembrane α_I helix, but the difference is not dramatic. For the third type of secondary structural element perpendicular to the membrane plane, α_{II} helix, β is about 110° (equivalent to 70°); this case is represented by the triangle in Figure 2b, and its predicted line shape is shown in Figure 4d. This provides a better fit to the peak of the experimental spectrum than does the α_I helix, but the fit to the edges of the spectrum is worse.

It is clear from Figure 4b–d that the shape of the experimental spectrum cannot be reproduced with a single tensor orientation, which is not surprising since it in principle contains 36 components. Although a unique fit of the spectrum cannot be expected, it is still useful to examine the effects on the line shape of tilting the secondary structural elements in the plane of the membrane. Tilting a helix will remove the rotational degeneracy so that now up to 18 different sets of angles will be present, depending on the helix length. Thus, for an α_I helix, tilting by x degrees from the membrane normal results in a spectrum which is the sum of a number of different subspectra, with the individual Euler angles ranging between $\beta = 90° \pm x°$ and $\alpha = 115° \pm x°$. In Figure 2b, the dotted lines trace out the positions of the subspectra for tilt angles of 10° and 20°. Figure 4e shows an approximation of the line shape for an α_I helix tilted at 20°, using eight subspectra; this fits quite well to the experimental line shape. For α_{II} helix, however, tilting moves the peak of the predicted line shape too far to the left, giving a worse fit to the experimental line shape than does the untilted α_{II} helix; this is shown in Figure 4f for α_{II} helix tilted by 10° from the membrane normal.

For β sheet, on the other hand, tilting the sheet axis away from the membrane normal generally yields a sum of two subspectra, and the effect depends on the direction of tilt. For tilt about the y axis of Figure 3b, the $\Delta\sigma$'s for the two subspectra diverge rapidly, moving in opposite directions as shown by the squares and diamonds in Figure 2c and the line shape of Figure 4g. Clearly, models with such tilts do not agree well with the experimental data. Tilting about the x axis of Figure 3c also yields a sum of two subspectra, but the differences between them are smaller than for the other direction of tilt. In Figure 2c, each such tilt gives two components which fall on the two dotted lines and are vertically displaced from each other; they have equivalent values for β but different values for α. At the extreme tilt of 90°, again both sets of peptide groups give the same $\Delta\sigma$ value; this case is represented by the triangle in Figure 2c. The $\Delta\sigma$ value for this case is quite close to that for the transmembrane α_I helix, and thus, models for BR consisting entirely of antiparallel β sheet with their axes close to parallel to the membrane plane would be just as consistent with the present experimental data as are models consisting entirely of helices with their axes close to perpendicular to the membrane plane. However, such an orientation is inconsistent with a large body of structural data for BR, in particular proteolytic digestion studies and electron microscopy, and will not be discussed further.

Jap et al. (1983) have suggested that BR contains several β-sheet strands tilted at about 10–15° from the membrane normal in the direction just discussed (about the x axis of Figure 3c). Shown in Figure 4h is the predicted line shape for a sum of 10° and 20° tilts (still about the x axis in Figure 3c); this shows a better fit to the experimental line shape than does β sheet tilted as first discussed above but does not fit as well as untilted or moderately tilted helices. Thus, if BR consists entirely of one secondary structural type at one tilt angle to the membrane normal, the above analysis would support only a model consisting of α_I helix tilted at about 20° to the membrane normal.

Since the three-dimensional models from electron microscopy clearly indicate the presence of both tilted and untilted structural elements, such models, as well as those containing

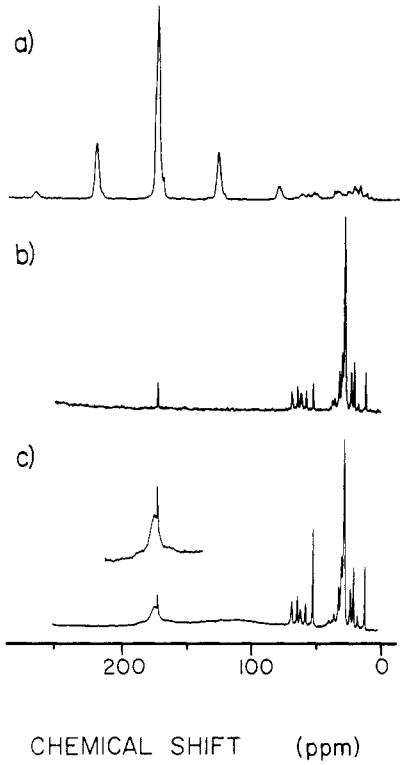

FIGURE 5: Magic-angle sample spinning (MASS) ^{13}C NMR spectra. (a) Cross-polarization spectrum of hydrated native purple membrane at a temperature of approximately 30 °C. Mixing time = 2 ms, recycle delay = 4 s, ν_R = 3.73 kHz. (b) Spectrum of reconstituted vesicles taken with cross-polarization as in (a) but with ν_R = 915 Hz. (c) Spectrum of reconstituted vesicles taken with a single 90° (^{13}C) pulse. The proton spins were kept saturated by applying a 90° proton pulse every 0.5 ms during the recycle delay. Recycle delay = 20 s, ν_R = 915 Hz.

more than one secondary structural type, must also be considered. Therefore, Figure 4i–4l presents the predicted line shapes for several such models. Figure 4i shows the case closest to the most generally accepted model, which is all α_I helix with three helices exactly parallel to the membrane normal, two tilted at 10°, and two tilted at 20°. Figure 4j shows the same model but with α_{II} helices. As examples of mixed structures, Figure 4k presents the line shape for a model in which 60% is α_I helix oriented parallel to the membrane normal and 40% is β sheet tilted as in Figure 4h at 10–20° from the membrane normal (half at 10° and half at 20°). Finally, Figure 4l shows the same case but with α_{II} helix instead of α_I helix. The line shape of Figure 4l fits the experimental spectrum almost as well as does that of Figure 4e. Thus, on the basis of this analysis, we cannot exclude the presence of 30–40% moderately tilted β sheet, particularly when coupled with α_{II} rather than α_I helix.

Magic-Angle Sample Spinning Spectra. A series of spectra of hydrated [^{13}C]leucine-labeled native purple membrane were taken by using magic-angle sample spinning (MASS) with cross-polarization, and an example is shown in Figure 5a. Some chemical shift heterogeneity is present, and the center band is about 3 ppm wide at half-height. At the right edge of the center band, almost resolved from it, is a line apparently due to a single carbonyl carbon; this is at −5 ppm from the maximum of the center band.

The reconstituted vesicles were also examined by MASS, and Figure 5b shows the spectrum obtained by cross-polarization, using the same mixing time as for the native membrane, at a temperature of approximately 30 °C. The only signal observed in the low-field region is that of the DMPC carbonyls at natural abundance (173 ppm), and all other major peaks can also be assigned to DMPC. Three minor peaks at 19, 37, and 39 ppm are probably due to the dihydrophytol chains of the purple membrane lipids; they correspond to those assigned to the branch methyls, C14, and the even carbons C2–12, respectively, according to Degani et al. (1980). Although it accounts for a large fraction of the ^{13}C present, the leucine carbonyl resonance is not visible. In contrast, in the Bloch decay MASS spectrum in Figure 5c, the BR carbonyls are observed as a broad peak underlying and slightly downfield of the sharp lipid carbonyl resonance and with an integrated intensity 18 times it. The spinning speed was deliberately kept low (915 Hz), and weak rotational side bands incompletely resolved from the center band are present.

The protein carbonyl line width is 570 Hz, or 7.1 ppm, more than twice that in native purple membrane. Since any major change in the protein structure is unlikely, this increased line width must be due to the presence of motion at a rate comparable to the shift anisotropy. In this case, T_2 becomes short, and the line will not be narrowed by magic-angle spinning (Waugh, 1979). When diffusion is much faster than the spinning frequency, eq 28 of Suewlack et al. (1980) can be used to estimate τ_c. In this limit, it reduces to $1/T_2 = \Delta^2\pi^2\tau_c/15$, where Δ is the chemical shift anisotropy in the plane perpendicular to the diffusion axis and τ_c is the rotational correlation time. The line width at half-height, $\Delta\nu = 1/\pi T_2$, is then equal to $\Delta^2\pi\tau_c/15$. If we take $\Delta \simeq 12$ kHz and assume diffusion roughly about σ_{22} and an excess line width (due to rotational diffusion) of ~350 Hz, we obtain $\tau_c \simeq 10^{-5}$ s. This value is probably a slight overestimate, since dipolar contributions from ^1H and ^{14}N to the line width are not considered. Thus, the agreement with the rates [$\tau_c \simeq (2–3) \times 10^{-6}$ s] previously measured by Cherry and co-workers (Peters & Cherry, 1982; Cherry & Godfrey, 1981) is quite reasonable.

Both the excess line width and the correlation time inferred from it suggest that the rotational diffusion of BR does not quite satisfy the fast-limit condition $\tau_c << 13$ μs. However, the observed powder line shape (Figure 1d) cannot be satisfactorily simulated by using slower motional rates. The sample temperature was not precisely known in the MASS experiments, and it is possible that the temperature in this case was somewhat less than 30 °C, leading to a lower rotational diffusion rate of the protein.

The absence of protein signals in cross-polarization spectra can be explained by the fact that motion with a τ_c of 10^{-5} s will reduce the proton $T_{1\rho}$ so that cross-polarization cannot occur efficiently. A similar absence of protein resonances in MASS NMR spectra obtained from visual rhodopsin has been reported by Sefcik et al. (1984), and the present results clarify the reasons for this problem. The protein rotational diffusion prevents the complete narrowing of its resonances by sample spinning, and therefore, spectral lines from an unlabeled protein would be broadened and so low in intensity as to be undetectable. In addition, Figure 4b clearly shows that if cross-polarization were used, even a labeled protein would be difficult to observe. Thus, the anisotropic motion of BR in its fluid lipid environment, which we have exploited in the powder NMR experiments discussed earlier, abates the usual advantages of MASS, i.e., high resolution. In order to recover the resolution, it would be necessary to adjust the experimental parameters so that the protein motion is either in the slow- or in the fast-limit regime.

Discussion

From analysis of the NMR powder line shapes of [1-^{13}C]leucine-labeled bacteriorhodopsin (BR), both in native

purple membrane and in reconstituted vesicles, several conclusions can be drawn. First, in native purple membrane, the peptide backbone of BR is rigid on the ^{13}C NMR time scale even at 40 °C, undergoing no motions with angular excursions >10° and faster than about 100 s^{-1}. The present results give no evidence for the mobility of surface residues of BR which Oldfield and co-workers have inferred from their deuterium NMR experiments (Keniry et al., 1981) (see discussion below). Second, in the reconstituted vesicles at 30 °C, the [^{13}C]leucine BR powder line shape is narrowed by rotational diffusion, which appears to be at a rate close to the fast limit (τ_c << 13 μs in this case). This motionally averaged line shape can be used to determine the range of orientations of the leucine peptide bonds relative to the diffusion axis, and a wide range of orientations can be excluded by comparison of theoretical and experimental line shapes.

Implicit in this analysis is the assumption that there are no major changes in the structure of BR when it is removed from its native membrane and put into DMPC vesicles. Monomeric BR in DMPC vesicles pumps protons (Dencher & Heyn, 1979; Bamberg et al., 1981) and exhibits the same photocycle intermediates as in native purple membrane (Dencher et al., 1983). However, its optical absorption maximum is slightly blue shifted (Cherry et al., 1978; Lewis & Engelman, 1983), and the rate and extent of light–dark adaption of BR are different in the two cases (Dencher et al., 1983). Thus, although there are unlikely to be any major structural differences between BR in the reconstituted vesicles and native purple membrane, one cannot rule out the possibility of small perturbations such as slight changes in tilt angles of the helices.

In the present case, the experimental line shape is not reproduced well by any single tensor orientation, but it can be simulated by two of the models considered here. The first of these consists entirely of α_I helices which are tilted at 20° from the membrane normal. The second is a combination of 60% α_{II} helix and 40% antiparallel β sheet; in this case, the helices are parallel to the membrane normal while the β-sheet strands are tilted half at 10° and half at 20°. Because of the axial asymmetry of the $^{13}C{=}O$ tensor, a given line shape can generally be fitted by a range of pairs of Euler angles. Thus, in the present case, although a wide range of Euler angles can be excluded, the cases which are consistent with other structural data give ^{13}C NMR line shapes which do not differ dramatically from each other. On the other hand, the advantage of using a label for which the rigid-lattice tensor is axially asymmetric is that for all possible orientations, the experimental line shape will clearly show whether fast motional averaging is, in fact, occurring. This is not the case for a tensor which is axially symmetric even when rigid; in this case, fast motion with $\beta = 0°$ has no effect on the line shape. Thus, the present experiments clearly demonstrate that rotational diffusion of BR occurs in the reconstituted vesicles and is fast relative to the width of the $^{13}C{=}O$ tensor.

These experiments also illustrate some of the difficulties which can arise in the application of solid-state NMR methods to semisolid samples such as fluid biological membranes. Cross-polarization is useful to provide increased sensitivity when BR is immobilized, both in the native purple membrane and in the reconstituted vesicles below the lipid phase transition temperature (T_m), but becomes much less efficient in the vesicles above T_m, due to the motion of the protein. In both static and MASS NMR experiments, little or no protein carbonyl intensity was observed in the cross-polarization spectra at a mixing time of 2 ms. In addition, even when the carbonyl peak was observed in a MASS experiment, it was much broader (7 vs. 3 ppm) than in the native membrane. Thus, the rotational motion of the protein prevents complete averaging of the chemical shift tensor by MASS. On the other hand, this residual line broadening can be used to estimate the rate of rotational diffusion, as shown by Suwelak et al. (1980).

The most general result of these experiments is the demonstration that information on the orientation of labeled groups relative to the plane of the membrane can be obtained for fluid membrane systems which are not amenable to macroscopic orientation. With ^{13}C or other isotopic labels, the application of these solid-state NMR methods to other membrane proteins may prove useful in testing structural models based on other information, especially for proteins which can neither be crystallized nor be completely dissolved.

It has recently been suggested that the surface residues of BR in *native* purple membrane, i.e., those residues in the loops as well as in the C-terminal and N-terminal tails, are highly mobile and are capable of executing essentially isotropic reorientation. This suggestion arises from the observation of sharp components in the ^2H spectra of BR containing ^2H-labeled amino acids (Keniry et al., 1984), and similar results were recently obtained from [1-^{13}C]Leu-labeled BR samples (E. Oldfield, unpublished results). However, in this laboratory, neither ^2H NMR spectra of ^2H-labeled BR (D. M. Rice, B. A. Lewis, J. Herzfeld, and R. G. Griffin, unpublished results) nor the [^{13}C]Leu spectra described here have revealed sharp spectral features which can be ascribed to isotropic motion. One possible explanation for this difference is that our membrane samples are aggregated and therefore the motion of the surface residues is restricted. It has been suggested that mild proteolytic digestion, i.e., loss of the C terminus in BR, promotes such aggregation (Keniry et al., 1984). However, electron microscope analysis of the native ^{13}C-labeled samples used here revealed that the membrane fragments were mostly (>80%) monodisperse, and in cases where aggregation was present, the overlap between the fragments was only partial rather than complete (see Materials and Methods). Furthermore, SDS gel electrophoresis of the NMR samples showed a single band at the correct position for intact BR, demonstrating that no significant proteolysis has occurred. Thus, these two biochemical assays do not support the notion that aggregation and/or proteolysis are responsible for the absence of the sharp components described by Keniry et al. Furthermore, the protein present in the samples of BR reconstituted into DMPC is clearly not aggregated—it is diffusing about the normal to membrane bilayers—and ^{13}C spectra of these samples do not reveal sharp components. Specifically, the line shape obtained from the static sample can be simulated satisfactorily by assuming the presence of α helices tilted with respect to the bilayer (Figure 1d). Furthermore, if there were isotropic components present in the samples, then additional sharp lines should be present in the MASS spectra of Figure 5. Presumably, the dynamic properties of these residues would satisfy fast-limit conditions, and they should lead to an additional sharp line in Figure 5 at 176 ppm, the isotropic shift obtained for [1-^{13}C]Leu in the native membrane MASS spectrum. This sharp line should be superimposed on the broad [1-^{13}C]Leu component and should be clearly resolved from the lipid C=O line at 173 ppm (line width 0.25 ppm). At the moment, we cannot satisfactorily explain these discrepancies between our results and those of Keniry et al.

ACKNOWLEDGMENTS

We are grateful to Dr. Mark Dumont for performing SDS gel electrophoresis on purple membrane samples. We also

thank Barry Stein for assistance with the electron microscopy and James Courtemanche and Cynthia Mulliken for the preparation and analysis of labeled purple membrane.

REFERENCES

Argade, P. V., Rothschild, K. J., Kawamoto, A. H., Herzfeld, J., & Herlihy, W. C. (1981) *Proc. Natl. Acad. Sci. U.S.A. 78*, 1643.

Bamberg, E., Dencher, N. A., Fahr, A., & Heyn, M. P. (1981) *Proc. Natl. Acad. Sci. U.S.A. 78*, 7502.

Cherry, R. J., & Godfrey, R. E. (1981) *Biophys. J. 36*, 257.

Cherry, R. J., Muller, U., & Schneider, G. (1977) *FEBS Lett. 80*, 465.

Cherry, R. J., Muller, U., Henderson, R., & Heyn, M. P. (1978) *J. Mol. Biol. 121*, 283.

Cross, T. A., & Opella, S. J. (1982) *J. Mol. Biol. 159*, 543.

Cross, T. A., & Opella, S. J. (1983) *J. Am. Chem. Soc. 105*, 306.

Degani, H., Danon, A., & Caplan, S. R. (1980) *Biochemistry 19*, 1626.

Dencher, N. A., & Heyn, M. P. (1979) *FEBS Lett. 108*, 307.

Dencher, N. A., & Heyn, M. P. (1983) *Biochemistry 22*, 1323.

Eads, T. M., & Mandelkern, L. (1984) *J. Biol. Chem. 259*, 10689.

Edidin, M. (1974) *Annu. Rev. Biophys. Bioeng. 3*, 179.

Engelman, D. M., Goldman, A., & Steitz, T. A. (1982) *Methods Enzymol. 88*, 81.

Griffin, R. G., Powers, L., & Pershan, P. S. (1978) *Biochemistry 17*, 2718.

Henderson, R. (1977) *Annu. Rev. Biophys. Bioeng. 6*, 87.

Henderson, R., & Unwin, P. N. T. (1975) *Nature (London) 257*, 28.

Herzfeld, J., & Berger, A. E. (1980) *J. Chem. Phys. 73*, 6021.

Hoffman, W., Restall, C. J., Hyla, R., & Chapman, D. (1980) *Biochim. Biophys. Acta 602*, 531.

Jap, B. K., Maestre, M. J., Hayward, S. B., & Glaeser, R. M. (1983) *Biophys. J. 43*, 81.

Keniry, M. A., Gutowsky, H. S., & Oldfield, E. (1984) *Nature (London) 307*, 383.

Khorana, H. G., Gerber, G. E., Herlihy, W. C., Gray, C. P., Anderegg, R. J., Nihei, K., & Bieman, K. (1979) *Proc. Natl. Acad. Sci. U.S.A. 76*, 5046.

Krimm, S., & Dwivedi, A. M. (1982) *Science (Washington, D.C.) 216*, 407.

Lewis, B. A., & Engelman, D. M. (1983) *J. Mol. Biol. 166*, 203.

Mehring, M. (1983) *High Resolution NMR in Solids*, Chapter 2, Springer-Verlag, West Berlin.

Mehring, M., Griffin, R. G., & Waugh, J. S. (1971) *J. Chem. Phys. 55*, 746.

Oesterhelt, D., & Stoeckenius, W. (1974) *Methods Enzymol. 31*, 667.

Ovchinnikov, Y. A., Abdulaev, N. G., Feigina, M. Y., Kiselev, A. V., & Lobanov, N. A. (1979) *FEBS Lett. 100*, 219.

Pauls, K. P., MacKay, A. L., Soderman, O., Bloom, M., Tanjea, A. K., & Hodges, R. S. (1985) *Eur. J. Biophys. 12*, 1.

Peters, R., & Cherry, R. J. (1982) *Proc. Natl. Acad. Sci. U.S.A. 79*, 4317.

Pines, A., Gibby, M. G., & Waugh, J. S. (1972) *Chem. Phys. Lett. 15*, 373.

Razi-Naqvi, K., Gonzalez-Rodriguez, J., Cherry, R. J., & Chapman, D. (1973) *Nature (London) 245*, 249.

Rothschild, K. J., Sanches, R., & Clark, N. A. (1982) *Methods Enzymol. 88*, 696.

Sarkar, S. K., Sullivan, C. E., & Torchia, D. A. (1983) *J. Biol. Chem. 258*, 9762.

Sefcik, M. D., Schaefer, J., Stejskal, E. O., McKay, R. A., Ellena, J. F., Dodd, W. S., & Brown, M. F. (1983) *Biochem. Biophys. Res. Commun. 114*, 1048.

Stark, R. E., Jelinski, L. W., Ruben, D. J., Torchia, D. A., & Griffin, R. G. (1983) *J. Magn. Reson. 55*, 266.

Stoeckenius, W., & Bogomolni, R. A. (1982) *Annu. Rev. Biochem. 52*, 587.

Suwelak, D., Rothwell, W. P., & Waugh, J. S. (1980) *J. Chem. Phys. 73*, 2559.

Szeverenyi, N. M., Sullivan, M. J., & Maciel, G. E. (1982) *J. Magn. Reson. 47*, 462.

Torchia, D. A., & Szabo, A. (1982) *J. Magn. Reson. 49*, 107.

Wagner, G., & Wüthrich, K. (1982) *J. Mol. Biol. 135*, 347.

Wallace, B. A. (1982) *Methods Enzymol. 88*, 447.

Waugh, J. S. (1979) in *NMR and Biochemistry: A Symposium in Honor of Mildred Cohn* (Opella, S. J., & Lu, P., Eds.) Plenum Press, New York.